The Acute Inhibitory Effect of Iodide Excess on Sodium/Iodide Symporter Expression and Activity Involves the PI3K/Akt Signaling Pathway

Caroline Serrano-Nascimento, Silvania da Silva Teixeira, Juan Pablo Nicola, Renato Tadeu Nachbar, Ana Maria Masini-Repiso, and Maria Tereza Nunes

Department of Physiology and Biophysics (C.S.-N., S.d.S.T., R.T.N., M.T.N.), Institute of Biomedical Sciences, University of São Paulo, 05508-000 São Paulo, Brazil; and Centro de Investigaciones en Bioquímica Clínica e Inmunología-Consejo Nacional de Investigaciones Científicas y Técnicas (J.P.N., A.M.M.-R.), Departamento de Bioquímica Clínica, Facultad de Ciencias Químicas, Universidad Nacional de Córdoba, X5000HUA Córdoba, Argentina

Iodide (I^-) is an irreplaceable constituent of thyroid hormones and an important regulator of thyroid function, because high concentrations of I^- down-regulate sodium/iodide symporter (NIS) expression and function. In thyrocytes, activation of phosphatidylinositol 3-kinase (PI3K)/protein kinase B (Akt) cascade also inhibits NIS expression and function. Because I^- excess and PI3K/Akt signaling pathway induce similar inhibitory effects on NIS expression, we aimed to study whether the PI3K/Akt cascade mediates the acute and rapid inhibitory effect of I^- excess on NIS expression/activity. Here, we reported that the treatment of PCCl3 cells with I^- excess increased Akt phosphorylation under normal or TSH/insulin-starving conditions. I^- stimulated Akt phosphorylation in a PI3K-dependent manner, because the use of PI3K inhibitors (wortmannin or 2-(4-Morpholinyl)-8-phenyl-4H-1-benzopyran-4-one) abrogated the induction of I^- effect. Moreover, I^- inhibitory effect on NIS expression and function were abolished when the cells were previously treated with specific inhibitors of PI3K or Akt (Akt1/2 kinase inhibitor). Importantly, we also found that the effect of I^- on NIS expression involved the generation of reactive oxygen species (ROS). Using the fluorogenic probes dihydroethidium and mitochondrial superoxide indicator (MitoSOX Red), we observed that I^- excess increased ROS production in thyrocytes and determined that mitochondria were the source of anion superoxide. Furthermore, the ROS scavengers N-acetyl cysteine and 2-phenyl-1,2-benzisoselenazol-3-(2H)-one blocked the effect of I^- on Akt phosphorylation. Overall, our data demonstrated the involvement of the PI3K/Akt signaling pathway as a novel mediator of the I^--induced thyroid autoregulation, linking the role of thyroid oxidative state to the Wolff-Chaikoff effect. (***Endocrinology*** **155: 1145–1156, 2014)**

Iodide (I^-) is essential for thyroid hormone biosynthesis. I^- is actively transported across the basolateral membrane of thyroid follicular cells by the sodium/iodide symporter (NIS), a plasma membrane glycoprotein that plays a critical role in thyroid physiology and pathophysiology (1, 2). NIS-mediated I^- uptake constitutes the first step in the biosynthesis of the only iodine-containing hormones in vertebrates, T_3 and T_4.

NIS expression in thyroid cells is regulated by several signal pathways, including the phosphatidylinositol 3-kinase (PI3K)/protein kinase B (Akt) pathway, which has an important role in the proliferation and differentiation of

ISSN Print 0013-7227 ISSN Online 1945-7170
Printed in U.S.A.

Received July 17, 2013. Accepted December 24, 2013.
First Published Online January 3, 2014

Abbreviations: Akt, protein kinase B; $Akti_{1/2}$, Akt1/2 kinase inhibitor; DHE, dihydroethidium; DMSO, dimethylsulfoxide; Ebselen, 2-phenyl-1,2-benzisoselenazol-3-(2H)-one; FBS, fetal bovine serum; GAPDH, glyceraldehyde 3-phosphate dehydrogenase; HA, hemagglutinin; HBSS, Hanks' balanced salt solution; H_2O_2, hydrogen peroxide; I^-, iodide; LY294002, 2-(4-morpholinyl)-8-phenyl-4H-1-benzopyran-4-one; MitoSOX Red, mitochondrial superoxide indicator; NAC, N-acetyl cysteine; NaI, sodium iodide; NHS-SS-biotin, succinimidyl 2-(biotinamido)-ethyl-1,3-dithiopropionate-biotin; NIS, sodium/iodide symporter; O_2^-, superoxide; PEG-SOD, superoxide dismutase-polyethylene glycol; PI3K, phosphatidylinositol 3-kinase; PTEN, phosphatase and tensin homolog; PTU, propylthiouracil; ROS, reactive oxygen species.

thyrocytes (3–5). Several studies have demonstrated that PI3K/Akt activation negatively regulates NIS function and expression in thyroid cells (6–9). Growth factors, such as insulin or IGF-I, activate PI3K and inhibit the TSH/cAMP-regulated I^- transport and NIS gene transcription (9, 10). Additionally, the use of selective PI3K inhibitors significantly increase NIS expression and function in thyrocytes (7–9, 11–13).

In addition to its essential role as a thyroid hormone constituent, I^- is one of the most important regulators of thyroid function. Since 1944 it is well known that I^- excess inhibits the biosynthesis and secretion of thyroid hormones (14). This phenomenon, known as the Wolff-Chaikoff effect (15), is transitory, and in rats, thyroid hormone biosynthesis and secretion are restored 2 days after I^- administration (16). The critical determinant for the Wolff-Chaikoff effect is the intracellular rather than the blood concentration of I^- (17). The "escape" of the Wolff-Chaikoff effect has been ascribed to an inhibition of NIS function (18–20). In fact, I^- excess inhibits NIS expression and activity, both at the transcriptional and posttranscriptional levels (21–26). Moreover, we recently reported that I^- excess promptly reduces NIS mRNA expression, stability, and translation efficiency both in vivo and in vitro (27, 28).

Although basal level of reactive oxygen species (ROS) production is important for maintaining thyroid hormone biosynthesis (29, 30), I^- excess increased production of ROS in thyrocytes (26, 31, 32). Several authors suggested that the increased generation of ROS triggered by I^- excess is responsible for its antiproliferative and cytotoxic effect on thyrocytes (29, 33, 34). Furthermore, the increased production of ROS has been associated to the activation of PI3K/Akt signaling pathway in different cellular lineages (35–39).

Because I^- excess and PI3K/Akt signaling pathway trigger similar inhibitory effects on NIS expression and activity in thyrocytes, this study aimed to investigate whether the PI3K/Akt cascade mediates the acute I^--induced NIS inhibition.

Materials and Methods

Reagents and antibodies

Bovine TSH, insulin, transferrin, hydrocortisone, protease inhibitor cocktail, Akt1/2 kinase inhibitor ($Akti_{1/2}$), wortmannin, 2-(4-morpholinyl)-8-phenyl-4H-1-benzopyran-4-one (LY294002), N-acetyl cysteine (NAC), 2-phenyl-1,2-benzisoselenazol-3-(2H)-one (Ebselen), dihydroethidium (DHE), superoxide dismutase-polyethylene glycol (PEG-SOD), antirabbit IgG-fluorescein isothiocyanate (FITC) antibody, and sodium iodide (NaI) were purchased from Sigma Chemical Co. Mitochondrial superoxide indicator (MitoSOX Red) was obtained from Molecular Probes. Affinity-purified polyclonal antirat NIS antibody was kindly provided by Dr Nancy Carrasco, as reported (40). Rabbit polyclonal antihemagglutinin (HA) antibody was purchased from Abcam. TRIzol, fetal bovine serum (FBS), OPTI-MEM, Platinum SYBR Green qPCR SuperMix, and LipofectAMINE 2000 reagent were from Invitrogen. Sulfo-succinimidyl 2-(biotinamido)-ethyl-1,3-dithiopropionate-biotin (NHS-SS-biotin) and streptoavidin agarose beads were purchased from Pierce Chemical Co. Polyclonal anti-Akt and antiphospho-Akt (Ser473) antibodies were from Cell Signaling Technology. Monoclonal anti-E-cadherin and anti-α-tubulin antibodies were from BD Transduction and Sigma Chemical Co, respectively. Enhanced

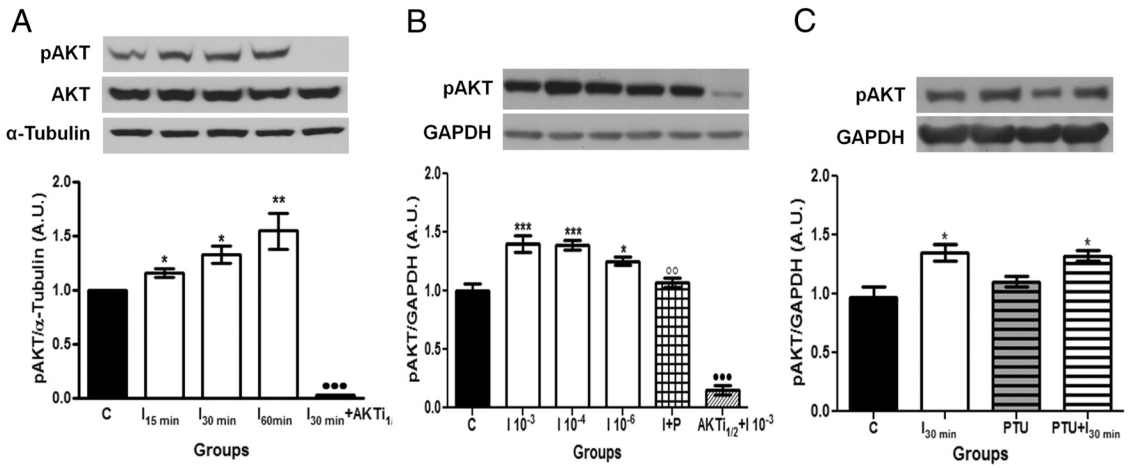

Figure 1. I^- excess induces Akt phosphorylation in PCCl3 cells. A, Western blot analysis of total or phosphorylated Akt in PCCl3 cells treated with 10^{-3}M NaI for different periods of time (15–60 min) or preincubated with the Akt inhibitor $Akti_{1/2}$ (10μM) for 1 hour before NaI treatment for 30 minutes. α-Tubulin was used for assessing of equal loading. B, Western blot analysis of Akt phosphorylation in PCCl3 cells treated with different concentrations of NaI (10^{-6}M to 10^{-3}M) or concomitantly treated with equal concentrations of NaI and $NaClO_4$ (I+P) for 30 minutes. GAPDH was used as loading control. C, Western blot analysis of Akt phosphorylation in PCCl3 cells preincubated with 1mM PTU for 1 hour before 10^{-3}M NaI treatment for 30 minutes. In all cases, immunoblots shown are representative of at least 3 independent experiments. Results are expressed as means ± SEM in arbitrary units (A.U.). *, $P < .05$; **, $P < .01$; ***, $P < .001$ vs control (C); °°, $P < .01$ vs I 10^{-3}, I 10^{-4}; ●●●, $P < .001$ vs $I_{15\ min}$, $I_{30\ min}$, $I_{60\ min}$, I 10^{-3}, I 10^{-4}, I 10^{-6} (ANOVA, Student-Newman-Keuls).

chemiluminescence kit was purchased from Amersham Biosciences. Monoclonal antiglyceraldehyde 3-phosphate dehydrogenase (GAPDH) and secondary horseradish peroxidase-conjugated antibodies were from Santa Cruz Biotechnology, Inc. I^- carrier-free $Na^{125}I$ was purchased from PerkinElmer.

Cell culture and treatments

PCCl3 thyroid cells were cultured in Ham's F12 medium supplemented with 5% FBS, 1-mU/mL bovine TSH, 10-μg/mL insulin, 5-μg/mL transferrin, and 10nM hydrocortisone at 37°C in a 95% air/5% CO_2 atmosphere. For experiments under starving conditions, PCCl3 cells at 70% confluence were shifted to the same medium without TSH and insulin, supplemented with 0.2% of FBS and cultured for 5 days before treatment (41, 42).

Cultured cells were treated with 10^{-3}M NaI (23, 25, 26) for 15, 30, and 60 minutes. Cells were also treated with different doses of NaI (10^{-3}M to 10^{-6}M) for 30 minutes. To evaluate the role of intracellular I^- excess, cells were concomitantly treated with equal concentrations of sodium iodide (10^{-3}M) and sodium perchlorate (10^{-3}M), a competitive NIS inhibitor (43, 44). To investigate the participation of the organified I^- in the induction of Akt phosphorylation, cells were incubated with 1mM propylthiouracil (PTU), which blocks I^- organification, for 1 hour before NaI treatment (10^{-3}M) for 30 minutes. When signaling pathways were studied, cells were preincubated with vehicle (dimethylsulfoxide [DMSO]) or specific inhibitors (10μM $Akti_{1/2}$, 0.5μM wortmannin, and 10μM LY294002) 1 hour before NaI treatment.

Transient transfection assays and efficiency analysis

PCCl3 cells cultured in starving medium for 3 days were transiently transfected with LipofectAMINE 2000 reagent following the manufacturer's recommendation. Briefly, cells seeded into 12-well dishes were transfected with HA-tagged rat NIS cDNA cloned into pcDNA3.1 vector (45). After transfection, cells were maintained in starving medium for 48 hours before NaI treatment.

The transfection efficiency was accessed by flow cytometry, as previously reported (45). Cells were fixed in 2% paraformaldehyde and stained with anti-HA tag antibody under nonpermeabilized conditions. Thereafter, the cells were incubated with an antirabbit IgG-fluorescein isothiocyanate (FITC) antibody. The fluorescence of 10^4 cells was assayed on a FACSCalibur flow cytometer. The results were evaluated using the Flowing Soft-

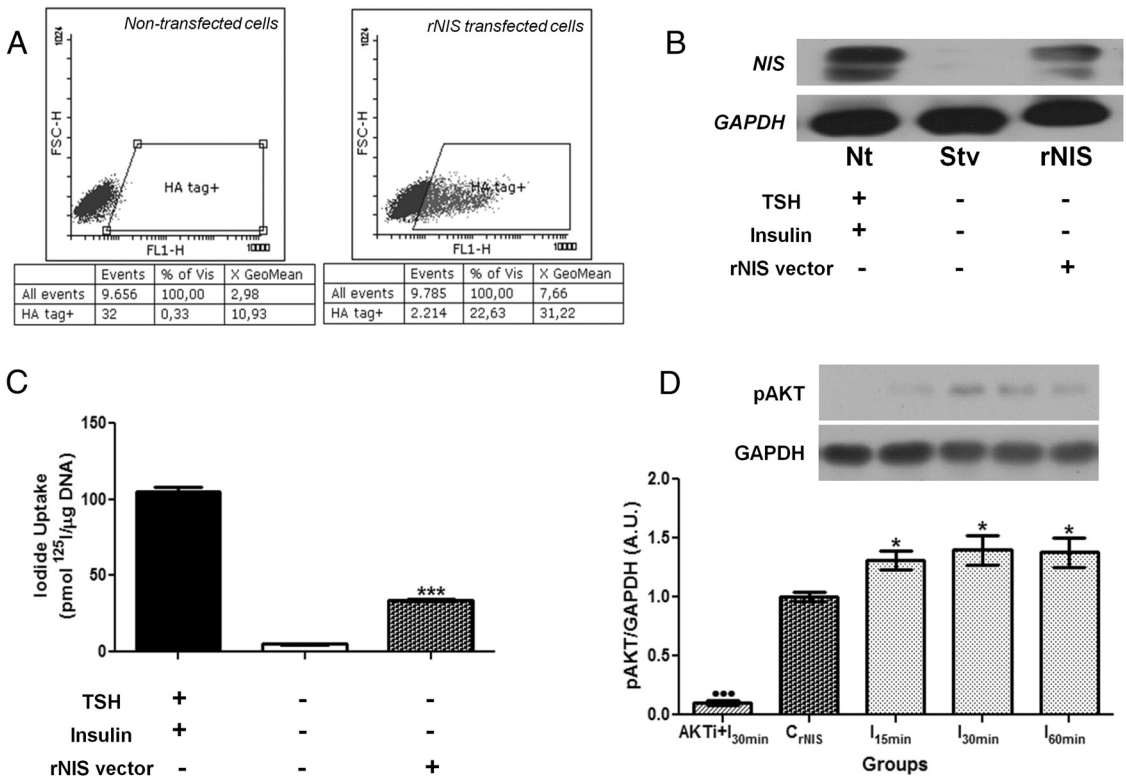

Figure 2. High concentration of I^- induces Akt phosphorylation in TSH/insulin-starved NIS-transfected PCCl3 cells. A, Transfection efficiency analysis performed by flow cytometry analysis under nonpermeabilized condition using an anti-HA antibody. B, Western blot analysis of total NIS expression. Immunoblots are representative of at least 3 independent experiments. GAPDH was used as loading control. Nt, nontransfected cells; Stv, cells starved for 5 days; rNIS, rat NIS-transfected cells starved for 5 days. C, Steady-state I^- uptake in starved PCCl3 either transfected or not with rat NIS cDNA. I^- uptake was expressed as pmol I^-/μg DNA. Each value represents the mean ± SEM of 3 independent experiments performed in triplicate. ***, $P < .005$ vs Stv (ANOVA, Student-Newman-Keuls). D, Western blot analysis of Akt phosphorylation in starved PCCl3 transiently expressing NIS cDNA treated with 10^{-3}M NaI for the indicated time points. One group of cells was preincubated with 10μM $Akti_{1/2}$ for 1 hour before NaI treatment (Akti+I_{30} min). GAPDH was analyzed as loading control. Immunoblots are representative of at least 3 independent experiments. Results are expressed as means ± SEM in arbitrary units (A.U.). *, $P < .05$ vs C rNIS; ●●●, $P < .001$ vs $I_{15\ min}$, $I_{30\ min}$, $I_{60\ min}$, and C rNIS (ANOVA, Student-Newman-Keuls). C rNIS, control PCCl3 expressing NIS cDNA.

ware 2.4.1 (Turku Centre for Biotechnology, University of Turku, Finland).

Measurement of intracellular superoxide (O_2^-) production

Detection of O_2^- generation in PCCl3 cells was performed using the O_2^- indicator DHE. Briefly, cells were incubated with 5μM DHE for 10 minutes before NaI treatment. Fluorescence was evaluated under a rhodamine filter in a ZEISS Axiovert 100M fluorescence microscope and Image-Pro Plus software. PEG-SOD enzyme (100 U/mL) was used to confirm that the red signal observed was related to O_2^- production (46).

To evaluate the role of ROS production on Akt phosphorylation, PCCl3 cells were pretreated with the nonspecific antioxidant NAC (1mM) (47), or the glutathione peroxidase mimetic Ebselen (30μM) (48), for 1 hour before NaI treatment.

Measurement of mitochondrial O_2^- production

O_2^- production was evaluated by flow cytometry and confocal fluorescence microscopy analysis using MitoSOX Red probe (49). Briefly, PCCl3 cells were treated with NaI and then incubated with 5μM MitoSOX Red probe for 20 minutes. The fluorescence of 10^4 events per sample was acquired using Guava easyCyte flow cytometer and analyzed with GuavaExpress Pro Software. Confocal microscopy analysis was performed on a Zeiss LSM 510 laser-scanning confocal microscope (Carl Zeiss).

RNA extraction and real-time PCR assay

Total RNA was extracted using TRIzol following the manufacturer protocol. NIS mRNA level was evaluated by real-time PCR, as previously described (27, 28). Real-time PCR amplifications were performed in duplicate using Platinum SYBR Green qPCR SuperMix-UDG. Gene-specific primers sequences are described in Supplemental Table 1, published on The Endocrine Society's Journals Online web site at http://endo.endojournals.org. Relative changes in NIS expression were calculated using the $2^{-\Delta\Delta Ct}$ method using ribosomal protein L19 as internal loading control. Analysis of melting curves resulted in a single peak for each pair of primers, indicating that a single PCR product was amplified.

Protein extraction and Western blot analysis

PCCl3 cells were lysed in an ice-cold homogenization solution containing 1% Triton X-100 in PBS supplemented with 1mM $NaOV_3$, 1mM NaF, 0.1mM phenylmethanesulfonyl fluoride, and protease inhibitor cocktail. Thirty micrograms of protein were diluted in loading buffer and boiled for 5 minutes. Proteins were resolved by 10% sodium dodecyl sulfate-PAGE and then transferred onto nitrocellulose membranes. Membranes were blocked and incubated with 1-μg/mL anti-phospho-Akt (Ser473) or 1-μg/mL anti-Akt antibodies. Equal loading was evaluated by stripping and reprobing the same membrane with 1-μg/mL anti-GAPDH or 0.2-μg/mL anti-α-tubulin antibodies. Blots were developed using the enhanced chemiluminescence kit. Blots densitometry was analyzed using the ImageJ software (National Institutes of Health).

Cell surface biotinylation

PCCl3 cells were washed with ice-cold PBS supplemented with 1mM $MgCl_2$ and 0.1mM $CaCl_2$ (PBS-CM) and incubated in 2mM $CaCl_2$, 150mM NaCl, and 20mM HEPES (pH 8.5) containing 1.0-mg/mL Sulfo-NHS-SS-biotin for 30 minutes at 4°C. Sulfo-NHS-SS-biotin excess was quenched in PBS-CM containing 100mM glycine. Cells were lysed in 50mM Tris-HCl (pH 7.5), 150mM NaCl, 5mM EDTA, 1% Triton X-100, 0.1% sodium dodecyl sulfate, and protease inhibitors; 150 μg of total protein were incubated overnight at 4°C with streptavidin agarose beads. Beads were washed, and adsorbed proteins were eluted with sample buffer at 75°C for 5 minutes. NIS content at the plasma membrane was analyzed by Western blotting, using 0.4-μg/mL anti-NIS antibody. Equal loading was evaluated by stripping and reprobing the same membrane with 0.2-μg/mL anti-E-cadherin antibody.

I^- uptake assay

I^- transport assays were performed as previously described (50). PCCl3 cells were treated with DMSO (vehicle), $Akti_{1/2}$ (10μM), LY294002 (10μM), or wortmannin (0.5μM) for 1 hour. Thereafter, the cells were incubated with 10^{-3}M sodium iodide for 30 minutes. Cells were washed 10 times with Hanks' balanced salt solution (HBSS) to remove any intracellular remaining free I^- and incubated with 20μM NaI supplemented with 50 μCi/μmol I^- carrier-free $Na^{125}I$ in HBSS for 30 minutes. Cells were washed twice with cold HBSS. The amount of $^{125}I^-$ accumulated in the cells was extracted with ice-cold ethanol and quantified in a γ-counter. For standardization, the DNA amount was determined by the diphenylamine method af-

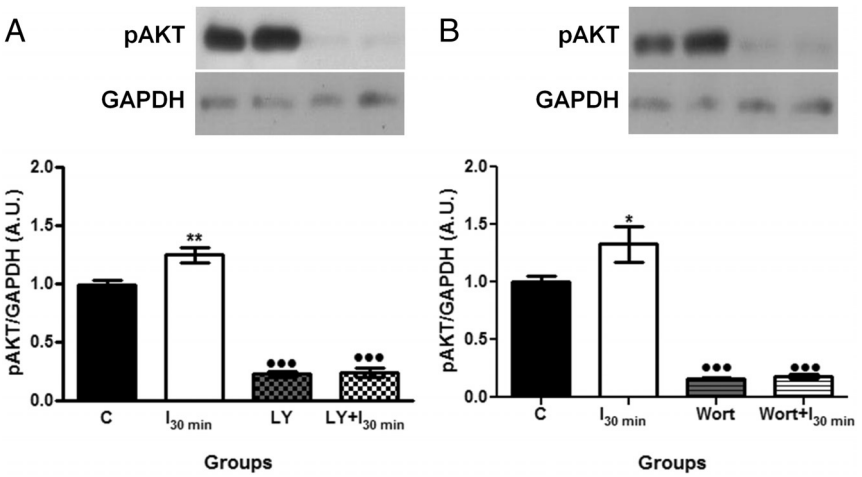

Figure 3. I^--induced Akt phosphorylation is PI3K dependent. Western blot analysis of Akt phosphorylation in PCCl3 cells preincubated with 10μM LY294002 (A) or 0.5μM wortmannin (B) for 1 hour before 10^{-3}M NaI treatment for 30 minutes. Equal loading was evaluated assessing GAPDH expression. Immunoblots shown are representative of at least 3 independent experiments. Results are shown as means ± SEM expressed in arbitrary units (A.U.). *, $P < .05$; **, $P < .01$ vs C; ●●●, $P < .001$ vs $I_{30\ min}$ and C (ANOVA, Student-Newman-Keuls). C, control group; LY, PCCl3 cells treated with 10 μM LY294002; Wort, PCCl3 cells treated with 0.5 μM Wortmannin.

ter trichloroacetic acid precipitation. Results were expressed as picomoles of I^- per μg DNA (pmol/μg DNA).

Statistical analysis

All data were reported as means ± SEM. Statistical analysis was performed by GraphPad Prism (GraphPad Software) from at least 3 independent experiments. Data were subjected to unpaired one-way ANOVA followed by Student-Newman-Keuls post hoc test. Differences were considered statistically significant at $P < .05$.

Results

I^- excess increases Akt phosphorylation

PI3K/Akt signaling pathway has been reported as a significant down-regulator of NIS gene expression in thyroid cells under different functional conditions (8, 9, 11). Therefore, we sought to study whether this signaling pathway is the mediator of decreased NIS expression induced by I^- excess in thyroid cells.

We examined Akt phosphorylation, a well-know target of PI3K, in I^- excess-treated thyroid cells. Incubation of PCCl3 cells with 10^{-3}M NaI significantly increased Ser473 Akt phosphorylation at all time points analyzed (15–60 min) (Figure 1A). I^- excess-induced Akt phosphorylation was completely abolished by the specific Akt inhibitor $Akti_{1/2}$ (Figure 1A). Total Akt levels were not changed by NaI treatment (Figure 1A).

We also observed that different concentrations of NaI (10^{-6}M to 10^{-3}M) induced Akt phosphorylation, although 10^{-3}M presented the most prominent induction (Figure 1B). This effect was abolished in the presence of the competitive NIS inhibitor perchlorate (Figure 1B).

Preincubation of PCCl3 cells with PTU has not altered the induction of Akt phosphorylation by NaI treatment (Figure 1C), suggesting that the effect of I^- does not require an organification step. Moreover, the effect of I^- on Akt phosphorylation was not related to a change in the osmolarity of the medium, because the treatment of PCCl3

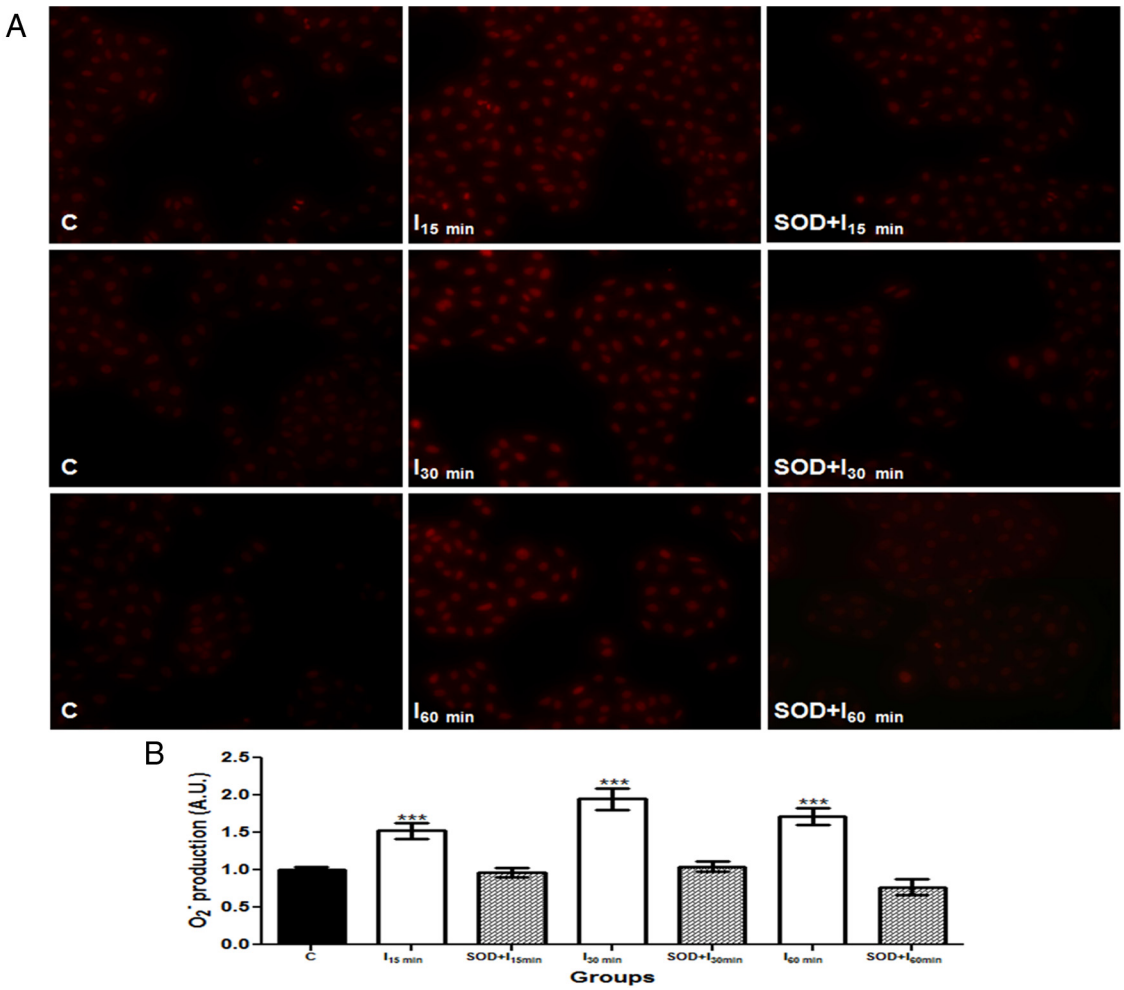

Figure 4. I^- excess induces ROS production. A, PCCl3 cells were treated with 10^{-3}M NaI during the indicated periods of time, and ROS production was evaluated using the fluorescent dye DHE (5μM). Specificity of ROS production was evaluated in the presence of 100-U/mL PEG-SOD (SOD). B, Relative quantification of O_2^- production in PCCl3 cells treated with 10^{-3}M NaI. Results are expressed as means ± SEM in arbitrary units (A.U.). Four independent experiments were performed, in triplicate. ***, $P < .001$ vs C (ANOVA, Student-Newman-Keuls). C, control group.

cells with 10^{-3}M NaCl has not induced Akt phosphorylation (Supplemental Figure 1).

In thyroid cells, Akt phosphorylation is stimulated by TSH or insulin/IGF-I treatment (9, 11). Therefore, we evaluated I^--induced Akt phosphorylation in PCCl3 cells cultured in the absence of TSH and insulin for 5 days (starved condition). Because NIS expression is severely reduced in the absence of TSH (51), PCCl3 cells were transiently transfected with NIS cDNA to ensure I^- accumulation. After transfection, we observed that 20%–25% of the transfected cell successfully expressed NIS at the plasma membrane (Figure 2A). Moreover, the partial recovery of NIS expression and activity was confirmed by Western blotting (Figure 2B) and $^{125}I^-$ uptake assay (Figure 2C). Interestingly, NaI treatment induced Akt phosphorylation, at all analyzed time points, even in the absence of TSH and insulin (Figure 2D). It is worth noting that under starved condition in non-NIS-transfected PCCl3 cells, NaI treatment was able to induce a minimal, although significant, Akt phosphorylation (Supplemental Figure 2).

PI3K-dependent I^--induced Akt phosphorylation

The canonical pathway for Akt phosphorylation involves the upstream activation of PI3K (52, 53). Therefore, we evaluated whether PI3K signaling is involved in the phosphorylation of Akt induced by I^- excess. PCCl3 cells were preincubated with the well-known PI3K inhibitors, wortmannin and LY294002 before NaI treatment. As shown in Figure 3, PI3K inhibition markedly reduced Akt phosphorylation in response to I^- excess, indicating that I^- induction of Akt phosphorylation is PI3K dependent.

I^--induced Akt phosphorylation relies on ROS production

Recently, Yao et al (32) demonstrated that high concentrations of I^- significantly increased ROS production in FRTL-5 thyroid cells. Therefore, we evaluated ROS production in PCCl3 cells in response to I^- excess and in shorter periods of time than the ones assessed before. As shown in Figure 4, the treatment of PCCl3 cells with NaI for 15–60 minutes increased the ROS production as evaluated by oxidation of the fluorescent indicator DHE. Preincubation of cells with PEG-SOD supported that NaI

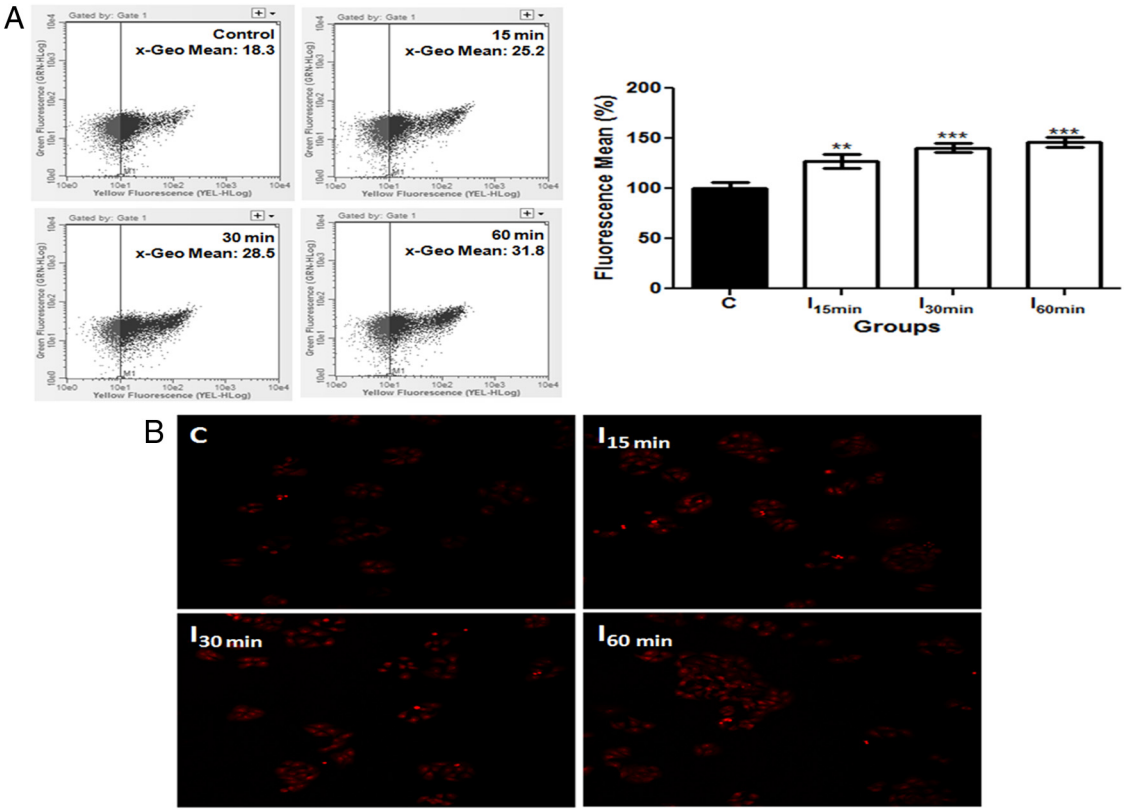

Figure 5. I^- excess induces mitochondrial O_2^- production. Mitochondrial O_2^- production was evaluated by using the mitochondrial superoxide indicator MitoSOX Red. A, left panel, Representative dot plots analysis of flow cytometry data obtained from cells incubated with 10^{-3}M NaI for 15, 30, and 60 minutes. Right panel, Relative quantification of fluorescence intensity means from flow cytometry data. Ten thousand events were evaluated per sample. Three independent experiments were performed in triplicate. **, $P < .01$; ***, $P < .001$ vs C (ANOVA, Student-Newman-Keuls). B, Evaluation of mitochondrial O_2^- production by confocal fluorescence microscope. Pictures are representative of 2 independent experiments performed in triplicate. C, control group.

treatment specifically increased O_2^- production, a precursor of hydrogen peroxide (H_2O_2) (Figure 4). Furthermore, we have observed that the treatment with lower doses of NaI (10^{-6}M and 10^{-4}M) also increased ROS production (Supplemental Figure 3). In addition, mitochondria seem to be the source of O_2^- production in PCCl3 cells exposed to I^- excess, as demonstrated by using the fluorogenic probe MitoSOX Red in flow cytometry (Figure 5A) and confocal fluorescence microscopy (Figure 5B) assays. As apoptosis interfere with mitochondrial function, we evaluated whether I^- excess affects PCCl3 cells viability or induces apoptosis. As shown in Supplemental Figure 4, NaI (10^{-3}M) treatment did not produce any significant effect on the analyzed parameters.

Thereafter, we evaluated the role of I^--induced ROS production on Akt phosphorylation. PCCl3 cells were incubated with NaI in the presence of ROS scavengers, NAC or Ebselen. As shown in Figure 6A, ROS scavengers impaired the induction of Akt phosphorylation by NaI treatment (Figure 6A). Ebselen treatment also reduced the I^--induced Akt phosphorylation in NIS-transfected PCCl3 cells cultured in starving medium for 5 days (Figure 6B).

PI3K/Akt signaling pathway mediates I^--induced NIS down-regulation

Inhibition of NIS expression is one of the main effects of I^- excess in thyrocytes. Thus, we evaluated whether the PI3K/Akt signaling pathway was involved in the reduction of NIS mRNA levels induced by I^- excess. As expected, a rapid reduction of NIS mRNA content was observed in PCCl3 cells treated with 10^{-3}M NaI for 30 minutes, but interestingly, the effect of I^- excess was abolished in the presence of PI3K or Akt inhibitors (Figure 7).

Previous studies have reported that high concentrations of I^- reduce NIS content at the thyrocytes plasma membrane (26, 54). As such, we observed a significant and rapid decrease of NIS protein expression at the plasma membrane of thyroid cells in response to NaI treatment for 30 minutes (Figure 8, A and B). This effect was prevented when the PCCl3 cells were pretreated with the Akt inhibitor $Akti_{1/2}$ (Figure 8A) or the PI3K inhibitor wortmannin (Figure 8B).

Inhibition of I^- uptake by high concentrations of I^- seems to be an adaptive response to reduce the intracellular I^- content (18, 19). In agreement with a reduced expression of NIS at the plasma membrane, NaI treatment rapidly (30 min) decreased I^- uptake in thyrocytes, and this effect was abolished in the presence of PI3K/Akt inhibitors (Figure 8, C–E). Interestingly, our data also suggest that, at short periods of time, inhibition of PI3K/Akt signaling did not affect I^- uptake in control cells.

Discussion

I^- is one of the most important NIS regulators in thyrocytes, and several studies have investigated the mechanisms that underlie the reduction of NIS expression and activity in response to high I^- concentrations (19–26). Transcriptional repression induced by I^- has been postulated as responsible

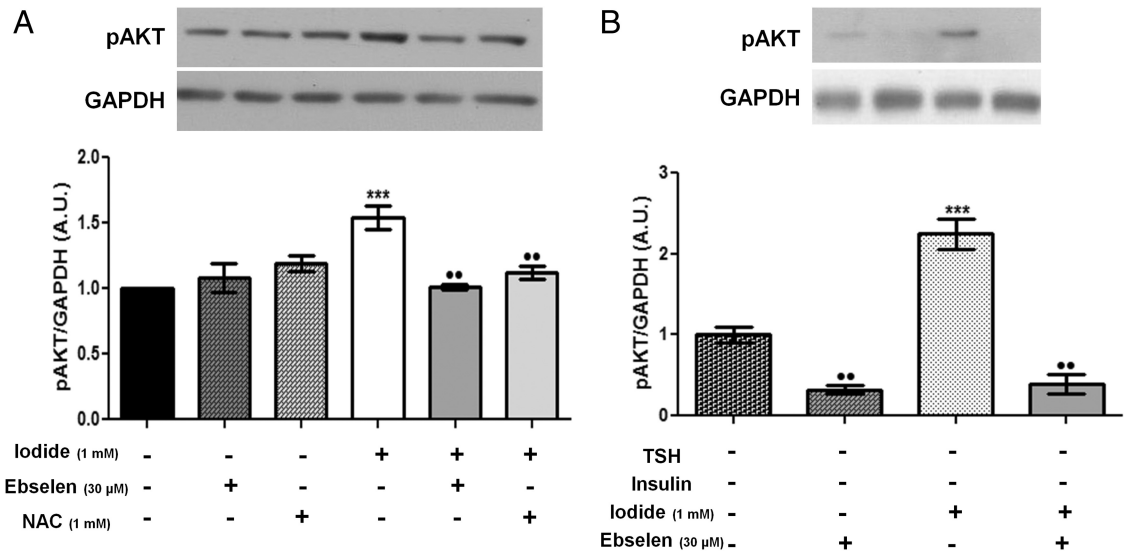

Figure 6. I^--induced ROS production increases Akt phosphorylation. A, Western blot analysis showing Akt phosphorylation in PCCl3 cells preincubated with 1mM NAC or 30μM Ebselen for 1 hour before 10^{-3}M NaI treatment for 30 minutes. GAPDH was used as loading control. B, Western blot analysis of Akt phosphorylation in rat NIS-transfected PCCl3 cells cultured under starving medium. Cells were preincubated with 30μM Ebselen for 1 hour and then treated with 10^{-3}M NaI for 30 minutes. Immunoblots shown are representative of at least 2 independent experiments. Results are expressed as means ± SEM in arbitrary units (A.U.). ***, $P < .001$ vs C; ●●, $P < .01$ vs $I_{30\ min}$ (ANOVA, Student-Newman-Keuls). C, control group.

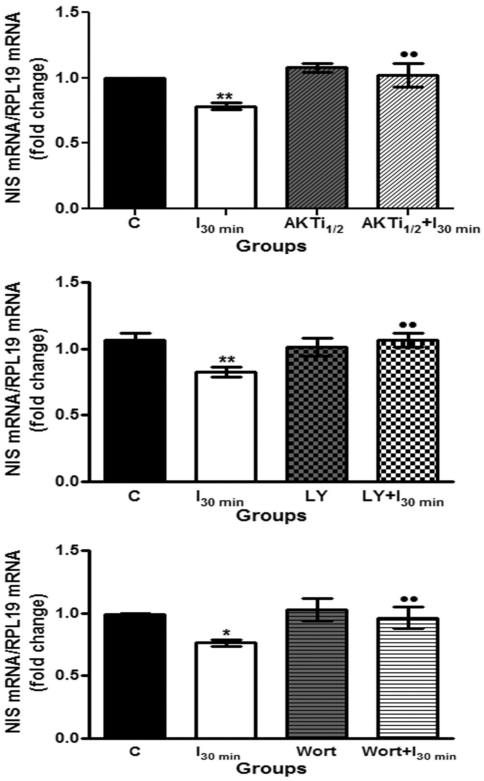

Figure 7. PI3K/Akt signaling pathway mediates I^--reduced NIS mRNA abundance. PCCl3 cells were preincubated with the Akt inhibitor $Akti_{1/2}$ (10μM), or the PI3K inhibitors LY294002 (10μM) and wortmannin (0.5μM) for 1 hour before NaI treatment (10^{-3}M) for 30 minutes. NIS mRNA levels relative to those of RPL19 were evaluated by real-time PCR. Values are indicated as fold change relative to the mRNA levels of cells treated with vehicle (DMSO). *, $P < .05$; **, $P < .01$ vs C; ●●, $P < .01$ vs $I_{30\ min}$ (ANOVA, Student-Newman-Keuls). C, control group; LY, PCCl3 cells treated with 10 μM LY294002; Wort, PCCl3 cells treated with 0.5 μM Wortmannin; RPL19, ribosomal protein L19.

for decreasing NIS mRNA levels in thyroid cells (22, 55). However, recent studies demonstrated that prompt posttranscriptional events, such as reduction of NIS mRNA stability and translation efficiency, are triggered in response to I^- administration (26–28, 56).

In this study, we demonstrated that the rapid inhibitory effect of high concentrations of I^- on NIS expression and function involve the participation of PI3K/Akt signaling pathway. In thyrocytes, PI3K/Akt signaling cascade has been associated with cell-cycle progression, cell survival, and differentiation (3–5, 57). However, the knowledge concerning PI3K/Akt pathway in regulating thyroid cell differentiation is still limited. Several studies have shown that PI3K/Akt pathway reduces TSH-stimulated NIS expression through transcriptional mechanisms (9, 11, 12). However, TSH, the main positive regulator of NIS expression in thyroid cells, activates PI3K/Akt signaling pathway through the binding on TSH receptor (6, 11). Stimulation of TSH receptor leads to the dissociation of trimeric G proteins into Gα and G$\beta\gamma$ subunits. The release of G$\beta\gamma$ dimmers stimulates PI3K/Akt signaling pathway in a cAMP-independent manner and down-regulates NIS gene expression by decreasing paired box gene 8 binding to the NIS promoter (11).

Our results demonstrated that I^- excess rapidly increased Akt phosphorylation in PCCl3 cells. This effect was observed even in the presence of low concentrations of I^- and in short periods of time. Although the important role of iodolipids on I^--induced effects in thyrocytes is well described (58), our results indicated that the iodolipids production through I^- organification may not be relevant for the induction of Akt phosphorylation by I^- excess. Moreover, the effect of I^- was dependent on intracellular I^- excess, because it was prevented by blocking I^- transport with perchlorate treatment (43, 44). We also evaluated whether I^- effects on Akt phosphorylation were dependent on TSH or insulin action. Our data demonstrated that NaI treatment has induced Akt phosphorylation even in the absence of both hormones, indicating a direct role of I^- on this cascade. In addition, we confirmed that I^--induced Akt phosphorylation was dependent on PI3K activity, because I^- effect was abolished when the cells were preincubated with PI3K inhibitors, wortmannin or LY294002.

Hyperactivity of PI3K/Akt signaling pathway has been implicated in the progression of thyroid cancer and correlates with reduced NIS expression at the plasma membrane (59–61). In addition, previous studies have demonstrated that PI3K/Akt cascade activation is involved in the internalization of proteins (62, 63). Furthermore, in breast carcinoma cells, PI3K signaling impairs NIS glycosylation and cell surface trafficking (64). In concordance, the blockage of PI3K signaling increased NIS targeting to the plasma membrane in normal and neoplastic thyrocytes (7). In agreement, here, we demonstrated that specific PI3K/Akt inhibitors abrogated the effects of I^- excess on NIS mRNA and plasma membrane expression. These data strongly suggest that the PI3K/Akt signaling pathway constitutes a novel mediator of the posttranscriptional effects induced by I^- excess.

The rapid reduction of NIS activity induced by I^- excess seems to be coherent, because I^- uptake is mainly mediated by NIS molecules placed at the plasma membrane (65). Moreover, the reduction of NIS activity observed when the intracellular concentration of I^- raises seems to be an efficient adaptation to prevent the deleterious effect of I^-. Interestingly, we observed that blockage of PI3K/Akt signaling pathway prevent the down-regulation of NIS function induced by I^-. Therefore, this signaling pathway participates in the adaptation mechanism of thyroid cells to I^- excess. Although we demonstrated that a reduction of NIS expression at the plasma membrane closely correlate with the reduction of NIS activity observed in

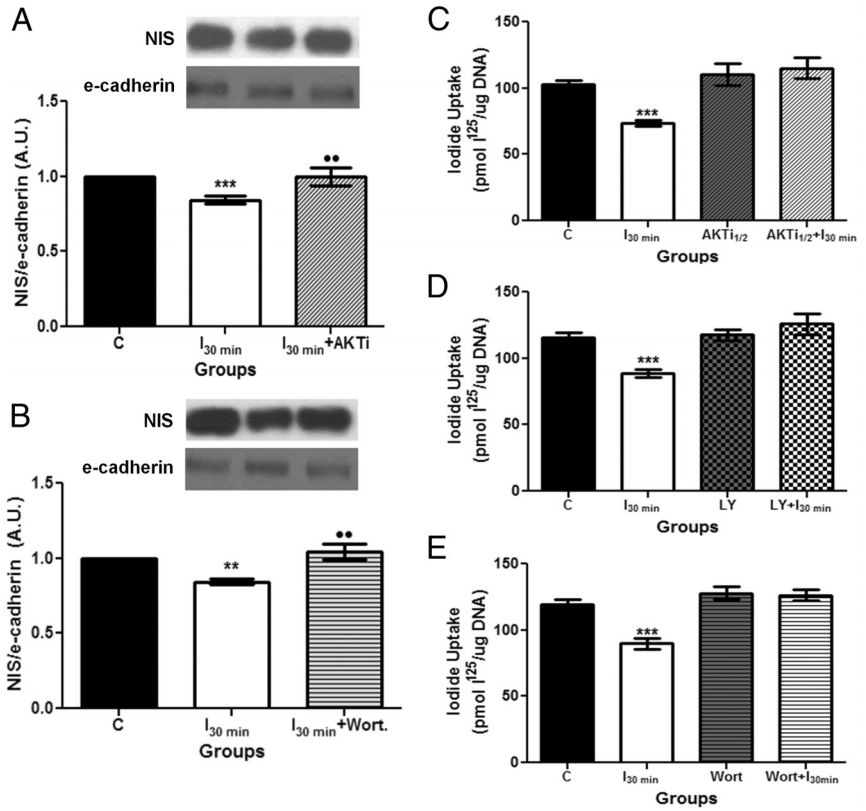

Figure 8. PI3K/Akt signaling pathway mediates I^--reduced NIS plasma membrane content and activity. PCCl3 cells were treated with 10μM $Akti_{1/2}$, 0.5μM wortmannin, or 10μM LY294002 for 1 hour before 10^{-3}M NaI treatment for 30 minutes. A and B, NIS expression at the plasma membrane was evaluated by cell surface biotinylation, followed by Western blot analysis. The plasma membrane marker E-cadherin was used as loading control. Immunoblots shown are representative of at least 3 independent experiments. Results are expressed as means ± SEM in arbitrary units (A.U.). **, $P < .01$; ***, $P < .001$ vs C; ●●, $P < .01$ vs $I_{30\ minutes}$ (ANOVA, Student-Newman-Keuls). C–E, Steady-state I^- uptake assay was performed in PCCl3 cells previously treated with $Akti_{1/2}$ (C), LY294002 (D), or wortmannin (E). I^- uptake was expressed as pmol I^-/μg DNA. Results are expressed as mean ± SEM of 3 independent experiments performed in triplicate. ***, $P < .001$ vs C; ●●●, $P < .001$ vs $I_{30\ min}$ (ANOVA, Student-Newman-Keuls). C, control group; LY, PCCl3 cells treated with 10 μM LY294002; Wort, PCCl3 cells treated with 0.5 μM Wortmannin.

response to NaI treatment, we do not discard that additional mechanisms might be involved in the regulation of NIS activity, such as inactivation of NIS molecules at the plasma membrane. Particularly, Leoni et al (26) predicted 2 intracellularly oriented and potentially redox-sensitive cysteine residues whose oxidation may result in a rapid inactivation of NIS protein.

NIS up-regulation induced by PI3K/Akt inhibition involves a transcriptional effect and, therefore, requires long periods of time to be observed (7–9). These results are consistent with our data, because the treatment of control PCCl3 cells with PI3K/Akt inhibitors for 1 hour did not alter NIS expression or activity. However, we have observed that the inhibitory effect of I^- excess on NIS was reversed by the preincubation of thyroid cells with PI3K/Akt inhibitors. Altogether, these data suggest that besides the well-described transcriptional events, the activation of PI3K/Akt signaling pathway is also involved in the I^--induced posttranscriptional events.

The mechanism by which I^- induced Akt phosphorylation in our experimental model was an intriguing issue. Previous studies have demonstrated that angiotensin I, cadmium, and other factors were able to induce PI3K/Akt signaling pathway in different cell lineages through the ROS production (35–39). In agreement, our data support the hypothesis that I^--induced ROS generation is crucial for stimulating Akt phosphorylation in thyrocytes, as pretreatment of PCCl3 cells with ROS scavengers, such as NAC or Ebselen, abrogated the effect of I^- on Akt phosphorylation.

ROS generation is extremely important for thyroid hormone biosynthesis, particularly H_2O_2, which plays an essential role in normal thyroid physiology, as a cofactor required for thyroid peroxidase-mediated I^- organification (66). The exposure of thyrocytes to I^- excess increases ROS production, intracellular oxidation levels, and therefore cell toxicity (29, 33, 34). However, the timing of I^--induced ROS generation is still controversy. Leoni et al (26) did not observe significant alteration on ROS production until 6 hours after I^- treatment, a modest effect after 24 hours (1.2-fold), reaching the maximum of ROS production at 48 hours. Nevertheless, the authors evaluated ROS production using the general oxidative stress indicator carboxy-2′,7′-dichlorodihydrofluorescein diacetate, which is not very sensitive to O_2^- anion (67). In sharp contrast, Yao et al (32) demonstrated increased mitochondrial O_2^- generation in FRTL-5 after 2 hours of I^- treatment, supporting our hypothesis that I^- could rapidly induce ROS production. In fact, posttranscriptional events are rapid and transiently elicited to keep cellular homeostasis, but they can be followed by different events that require longer periods of time to be triggered. Moreover, in agreement with Yao et al (32), our results demonstrated an impairment of ROS production in thyrocytes previously treated with PEG-SOD, suggesting that the source of ROS could be the mitochondria. In addition, the oxidation of

MitoSOX Red probe confirmed increased mitochondrial O_2^- production in response to NaI treatment.

It has been described that redox status interferes with the activity of several members of protein tyrosine phosphatases through the interaction with reactive cysteine residues (68–71). Phosphatase and tensin homolog (PTEN) is a well-known phosphoinositide-3-phosphatase that inhibits Akt activation (72). Several studies demonstrated that PTEN activity is regulated by different posttranslational mechanisms, as its inhibition through the reversible oxidation of catalytic cysteine residues in the presence of H_2O_2 (73, 74). Thus, we hypothesize that the increased ROS production induced by I^- might interfere with PTEN or other phosphatase activity leading to an increased Akt phosphorylation in thyrocytes. Therefore, these data reinforce the important role of thyroid redox state in the inhibition of NIS expression/activity induced by I^- excess (26).

In summary, our study points to a novel role of PI3K/Akt signaling pathway as a mediator of thyroid autoregulation induced by I^- and links the role of thyroid oxidative state to the Wolff-Chaikoff effect.

Acknowledgments

We thank Leonice L. Poyares for excellent technical assistance and Dr Nancy Carrasco (Yale University School of Medicine, New Haven, CT) for kindly providing affinity-purified antirat NIS antibody and HA-tagged rat NIS cDNA.

Address all correspondence and requests for reprints to: Maria Tereza Nunes, PhD, Full Professor, Department of Physiology and Biophysics, Institute of Biomedical Sciences, University of São Paulo, 05508-000 São Paulo, São Paulo, Brazil. E-mail: mtnunes@icb.usp.br.

This work was supported by Fundação de Amparo à Pesquisa do Estado de São Paulo Grants 2009/50175-6 (to C.S.-N.) and 2009/17834-6 (to M.T.N.), by grants from Fondo Nacional de Ciencia y Tecnología and Secretaría de Ciencia y Tecnología de la Universidad Nacional de Córdoba, and by Agencia Córdoba Ciencia (A.M.M.-R.).

Disclosure Summary: The authors have nothing to disclose.

References

1. **Carrasco N.** Iodide transport in the thyroid gland. *Biochem Biophys Acta*. 1993;1154:65–82.
2. **Dohán O, De la Vieja A, Paroder V, et al.** The sodium/iodide Symporter (NIS): characterization, regulation, and medical significance. *Endocr Rev*. 2003;24:48–77.
3. **Ciullo I, Diez-Roux G, Di Domenico M, Migliaccio A, Avvedimento EV.** cAMP signaling selectively influences Ras effectors pathways. *Oncogene*. 2001;20:1186–1192.
4. **Coulonval K, Vandeput F, Stein RC, Kozma SC, Lamy F, Dumont JE.** Phosphatidylinositol 3-kinase, protein kinase B and ribosomal S6 kinases in the stimulation of thyroid epithelial cell proliferation by cAMP and growth factors in the presence of insulin. *Biochem J*. 2000;348:351–358.
5. **Kimura T, Van Keymeulen A, Golstein J, Fusco A, Dumont JE, Roger PP.** Regulation of thyroid cell proliferation by TSH and other factors: a critical evaluation of in vitro models. *Endocr Rev*. 2001;22:631–656.
6. **Suh JM, Song JH, Kim DW, et al.** Regulation of the phosphatidylinositol 3-kinase, Akt/protein kinase B, FRAP/mammalian target of rapamycin, and ribosomal S6 kinase 1 signaling pathways by thyroid-stimulating hormone (TSH) and stimulating type TSH receptor antibodies in the thyroid gland. *J Biol Chem*. 2003;278:21960–21971.
7. **Kogai T, Sajid-Crockett S, Newmarch LS, Liu YY, Brent GA.** Phosphoinositide-3-kinase (PI3K) inhibition induces sodium/iodide symporter expression (NIS) in rat thyroid cells and human pappilary cancer cells. *J Endocrinol*. 2008;199:243–252.
8. **Liu YY, Zhang X, Ringel MD, Jhiang SM.** Modulation of sodium iodide symporter expression and function by LY294002, $Akti_{1/2}$ and rapamycin in thyroid cells. *Endocr Relat Cancer*. 2012;19:291–304.
9. **Garcia B, Santisteban P.** PI3K is involved in the IGF-I inhibition of TSH-induced sodium/iodide symporter gene expression. *Mol Endocrinol*. 2002;16:342–352.
10. **Saji M, Kohn LD.** Insulin and insulin-like growth factor-I inhibit thyrotropin-increased iodide transport in serum-depleted FRTL-5 rat thyroid cells: modulation of adenosine 3′,5′-monophosphate signal action. *Endocrinology*. 1991;128:1136–1143.
11. **Zaballos MA, Garcia B, Santisteban P.** G$\beta\gamma$ dimers released in response to thyrotropin activate phosphoinositide 3-kinase and regulate gene expression in thyroid cells. *Mol Endocrinol*. 2008;22:1183–1199.
12. **de Souza EC, Padrón AS, Braga WM, et al.** mTOR downregulates iodide uptake in thyrocytes. *J Endocrinol*. 2010;206:113–120.
13. **Hou P, Bojdani E, Xing M.** Induction of thyroid gene expression and radioiodine uptake in thyroid cancer cells by targeting major signaling pathways. *J Clin Endocrinol Metab*. 2010;95:820–828.
14. **Morton ME, Chaikoff IL, Rosenfeld S.** Inhibiting effect of inorganic iodide on the formation in vitro of thyroxine and diiodotyrosine by surviving thyroid tissue. *J Biol Chem*. 1944;154:381–387.
15. **Wolff J, Chaikoff IL.** Plasma inorganic iodide as a homeostatic regulator of thyroid function. *J Biol Chem*. 1948;174:555–564.
16. **Wolff J, Chaikoff IL, Goldberg RC, Meier JR.** The temporary nature of the innibitory action of excess iodide on organic iodine synthesis in the normal thyroid. *Endocrinology*. 1949;45:504–513.
17. **Raben MS.** The paradoxical effect of thiocyanate and of thyrotropin on the organic binding of iodine by the thyroid in the presence of large amounts of iodide. *Endocrinology*. 1949;45:296–304.
18. **Braverman LE, Ingbar SH.** Changes in thyroidal function during adaptation to large doses of iodide. *J Clin Invest*. 1963;42:1216–1231.
19. **Grollman EF, Smolar A, Ommaya A, Tombaccini D, Santisteban P.** Iodine suppression of iodide uptake in FRTL-5 thyroid cells. *Endocrinology*. 1986;118:2477–2482.
20. **Spitzweg C, Joba W, Morris JC, Heufelder AE.** Regulation of sodium iodide symporter gene expression in FRTL-5 rat thyroid cells. *Thyroid*. 1999;9:821–830.
21. **Uyttersprot N, Pelgrims N, Carrasco N, et al.** Moderate doses of iodide in vivo inhibit cell proliferation and the expression of thyroperoxidase and Na+/I- symporter mRNAs in dog thyroid. *Mol Cell Endocrinol*. 1997;131:195–203.
22. **Eng PH, Cardona GR, Fang SL, et al.** Escape from the acute Wolff-Chaikoff effect is associated with a decrease in thyroid sodium/iodide symporter messenger ribonucleic acid and protein. *Endocrinology*. 1999;140:3404–3410.
23. **Eng PH, Cardona GR, Previti MC, Chin WW, Braverman LE.** Reg-

ulation of the sodium iodide symporter by iodide in FRTL-5 cells. *Eur J Endocrinol*. 2001;144:139–144.
24. **Ferreira AC, Lima LP, Araújo RL, et al.** Rapid regulation of thyroid sodium-iodide symporter activity by thyrotrophin and iodine. *J Endocrinol*. 2005;184:69–76.
25. **Leoni SG, Galante PA, Ricarte-Filho JC, Kimura ET.** Differential gene expression analysis of iodide-treated rat thyroid follicular cell line PCCl3. *Genomics*. 2008;91:356–366.
26. **Leoni SG, Kimura ET, Santisteban P, De la Vieja A.** Regulation of thyroid oxidative state by thioredoxin reductase has a crucial role in thyroid responses to iodide excess. *Mol Endocrinol*. 2011;25:1924–1935.
27. **Serrano-Nascimento C, Calil-Silveira J, Nunes MT.** Posttranscriptional regulation of sodium-iodide symporter mRNA expression in the rat thyroid gland by acute iodide administration. *Am J Physiol Cell Physiol*. 2010;298:C893–C899.
28. **Serrano-Nascimento C, Calil-Silveira J, Goulart-Silva F, Nunes MT.** New insights about the posttranscriptional mechanisms triggered by iodide excess on sodium/iodide symporter (NIS) expression in PCCl3 cells. *Mol Cell Endocrinol*. 2012;349:154–161.
29. **Poncin S, Gérard AC, Boucquey M, et al.** 2008 Oxidative stress in the thyroid gland: from harmlessness to hazard depending on the iodine content. *Endocrinology*. 2008;149:424–433.
30. **Poncin S, Colin IM, Gérard AC.** Minimal oxidative load: a prerequisite for thyroid cell function. *J Endocrinol*. 2009;201:161–167.
31. **Vitale M, Di Matola T, D'Ascoli F, et al.** Iodide excess induces apoptosis in thyroid cells through a p53-independent mechanism involving oxidative stress. *Endocrinology*. 2000;141:598–605.
32. **Yao X, Li M, He J, et al.** Effect of early acute high concentrations of iodide exposure on mitochondrial superoxide production in FRTL cells. *Free Radic Biol Med*. 2012;52:1343–1352.
33. **Many MC, Mestdagh C, van den Hove MF, Denef JF.** In vitro study of acute toxic effects of high iodide doses in human thyroid follicles. *Endocrinology*. 1992;131:621–630.
34. **Golstein J, Dumont JE.** Cytotoxic effects of iodide on thyroid cells: difference between rat thyroid FRTL-5 cell and primary dog thyrocyte responsiveness. *J Endocrinol Invest*. 1996;19:119–126.
35. **Chen L, Xu B, Liu L, et al.** Cadmium induction of reactive oxygen species activates the mTOR pathway, leading to neuronal cell death. *Free Radic Biol Med Mar*. 2011;50:624–632.
36. **Ushio-Fukai M, Alexander RW, Akers M, et al.** Reactive oxygen species mediate the activation of Akt/protein kinase B by angiotensin II invascular smooth muscle cells. *J Biol Chem*. 1999;274:22699–22704.
37. **Son YO, Wang L, Poyil P, et al.** Cadmium induces carcinogenesis in BEAS-2B cells through ROS-dependent activation of PI3K/AKT/GSK-3β/β-catenin signaling. *Toxicol Appl Pharmacol*. 2012;264:153–160.
38. **Sadidi M, Lentz SI, Feldman EL.** Hydrogen peroxide-induced Akt phosphorylation regulates Bax activation. *Biochimie*. 2009;91:577–585.
39. **Dong-Yun S, Yu-Ru D, Shan-Lin L, Ya-Dong Z, Lian W.** Redox stress regulates cell proliferation and apoptosis of human hepatoma through Akt protein phosphorylation. *FEBS Lett*. 2003;542:60–64.
40. **Levy O, Dai G, Riedel C, et al.** Characterization of the thyroid Na+/I- symporter with an anti-COOH terminus antibody. *Proc Natl Acad Sci USA*. 1997;94:5568–5573.
41. **Nicola JP, Nazar M, Mascanfroni ID, Pellizas CG, Masini-Repiso AM.** NF-κB p65 subunit mediates lipopolysaccharide-induced Na(+)/I(-) symporter gene expression by involving functional interaction with the paired domain transcription factor Pax8. *Mol Endocrinol*. 2010;24:1846–1862.
42. **Sue M, Akama T, Kawashima A, et al.** Propylthiouracil increases sodium/iodide symporter gene expression and iodide uptake in rat thyroid cells in the absence of TSH. *Thyroid*. 2012;22:844–852.
43. **Wolff J.** Perchlorate and the thyroid gland. *Pharmacol Rev*. 1998;50:89–115.
44. **Dohán O, Portulano C, Basquin C, Reyna-Neyra A, Amzel LM, Carrasco N.** The Na+/I symporter (NIS) mediates electroneutral active transport of the environmental pollutant perchlorate. *Proc Natl Acad Sci USA*. 2007;104:20250–20255.
45. **Paroder-Belenitsky M, Maestas MJ, Dohán O, et al.** Mechanism of anion selectivity and stoichiometry of the Na+/I- symporter (NIS). *Proc Natl Acad Sci USA*. 2011;108:17933–17938.
46. **Zuo L, Christofi FL, Wright VP, et al.** Intra- and extracellular measurement of reactive oxygen species produced during heat stress in diaphragm muscle. *Am J Physiol Cell Physiol*. 2000;279:C1058–C1066.
47. **Cotgreave IA.** N-acetylcysteine: pharmacological considerations and experimental and clinical applications. *Adv Pharmacol*. 1997;38:205–227.
48. **Sies H.** Ebselen, a selenoorganic compound as glutathione peroxidase mimic. *Free Radic Biol Med*. 1993;14:313–323.
49. **Graciano MF, Valle MM, Curi R, Carpinelli AR.** Evidence for the involvement of GPR40 and NADPH oxidase in palmitic acid-induced superoxide production and insulin secretion. *Islets*. 2013;5(4):139–148.
50. **Nicola JP, Nazar M, Serrano-Nascimento C, et al.** Iodide transport defect: functional characterization of a novel mutation in the Na+/I-symporter 5′-untranslated region in a patient with congenital hypothyroidism. *J Clin Endocrinol Metab*. 2011;96:E1100–E1107.
51. **Riedel C, Levy O, Carrasco N.** Post-transcriptional regulation of the sodium/iodide symporter by thyrotropin. *J Biol Chem*. 2001;276:21458–21463.
52. **Cheng JQ, Lindsley CW, Cheng GZ, Yang H, Nicosia SV.** The Akt/PKB pathway: molecular target for cancer drug discovery. *Oncogene*. 2005;24:7482–7492.
53. **Fayard E, Tintignac LA, Baudry A, Hemmings BA.** Protein kinase B/Akt at a glance. *J Cell Sci*. 2005;118:5675–5678.
54. **Dohán O, De la Vieja A, Carrasco N.** Hydrocortisone and purinergic signaling stimulate sodium/iodide symporter (NIS)-mediated iodide transport in breast cancer cells. *Mol Endocrinol*. 2006;20:1121–1137.
55. **Suzuki K, Kimura H, Wu H, et al.** Excess iodide decreases transcription of NIS and VEGF genes in rat FRTL-5 thyroid cells. *Biochem Biophys Res Commun*. 2010;393:286–290.
56. **Nicola JP, Reyna-Neyra A, Carrasco N, Masini-Repiso AM.** Dietary iodide controls its own absorption through post-transcriptional regulation of the intestinal Na+/I- symporter. *J Physiol*. 2012;590:6013–6026.
57. **Cass LA, Summers SA, Prendegast GV, Backer JM, Birnbaum MJ, Meinkoth JL.** Protein kinase A-dependent and -independent signaling pathways contribute to cyclic AMP-stimulated proliferation. *Mol Cell Biol*. 1999;19:5882–5891.
58. **Dugrillon A.** Iodolactones and iodoaldehydes-mediators of iodine in thyroid autoregulation. *Exp Clin Endocrinol Diabetes*. 1996;104:41–45.
59. **Ringel MD, Hayre N, Saito J, et al.** Overexpression and overactivation of AKT in thyroid carcinoma. *Cancer Res*. 2001;61:6105–6111.
60. **Saji M, Ringel MD.** The PI3K-Akt-mTOR pathway in initiation and progression of thyroid tumors. *Mol Cell Endocrinol*. 2010;321:20–28.
61. **Xing M.** Genetic alterations in PI3K/Akt pathway in thyroid cancer. *Thyroid*. 2010;20:697–706.
62. **Botelho RJ, Tapper H, Furuya W, Mojdami D, Grinstein S.** Fc γ R-mediated phagocytosis stimulates localized pinocytosis in human neutrophils. *J Immunol*. 2002;69:4423–4429.
63. **Uriarte SM, Jog NR, Luerman GC, Bhimani S, Ward RA, Mcleish KR.** Counterregulation of clathrin-mediated endocytosis by the actin and microtubular cytoskeleton in human neutrophils. *Am J Physiol Cell Physiol*. 2009;96:C857–C867.
64. **Knostman KA, McCubrey JA, Morrison CD, Zhang Z, Capen CC, Jhiang SM.** PI3K activation is associated with intracellular sodium/iodide symporter protein expression in breast cancer. *BMC Cancer*. 2007;7:137.
65. **Kaminsky SM, Levy O, Salvador C, Dai G, Carrasco N.** Na(+)-I-symport activity is present in membrane vesicles from thyrotropin-

deprived non-I(-)-transporting cultured thyroid cells. *Proc Natl Acad Sci USA*. 1994;91:3789–3793.
66. **Song Y, Driessens N, Costa M, et al.** Roles of hydrogen peroxide in thyroid physiology and disease. *J Clin Endocrinol Metab*. 2007;92:3764–3773.
67. **Haughland R. Eugene, OR.** *Molecular Probes. Handbook of Fluorescent Probes and Research Chemicals*. 11th ed. Eugene, OR: Catalogue of Molecular Probes, Inc; 2009.
68. **Denu JM, Tanner KG.** Specific and reversible inactivation of protein tyrosine phosphatases by hydrogen peroxide: evidence for a sulfenic acid intermediate and implications for redox regulation. *Biochemistry*. 1998;37:5633–5642.
69. **Lee SR, Kwon KS, Kim SR, Rhee SG.** Reversible inactivation of protein-tyrosine phosphatase 1B in A431 cells stimulated with epidermal growth factor. *J Biol Chem*. 1998;273:15366–15372.
70. **Meng TC, Fukada T, Tonks NK.** Reversible oxidation and inactivation of protein tyrosine phosphatases in vivo. *Mol Cell*. 2002;9:387–399.
71. **Downes CP, Walker S, McConnachie G, Lindsay Y, Batty IH, Leslie NR.** Acute regulation of the tumour suppressor phosphatase, PTEN, by anionic lipids and reactive oxygen species. *Biochem Soc Trans*. 2004;32:338–342.
72. **Maehama T, Dixon JE.** The tumor suppressor, PTEN/MMAC1, dephosphorylates the lipid second messenger, phosphatidylinositol 3,4,5-trisphosphate. *J Biol Chem*. 1998;273:13375–13378.
73. **Lee SR, Yang KS, Kwon J, Lee C, Jeong W, Rhee SG.** Reversible inactivation of the tumor suppressor PTEN by H2O2. *J Biol Chem*. 2002;277:20336–20342.
74. **Leslie NR, Bennett D, Lindsay YE, Stewart H, Gray A, Downes CP.** Redox regulation of PI 3-kinase signalling via inactivation of PTEN. *EMBO J*. 2003;22:5501–5510.

Supplemental Material Manuscript EN-13-1665R1

"The acute inhibitory effect of iodide excess on sodium/iodide symporter expression and activity involves the PI3K/Akt signaling pathway" by Caroline Serrano-Nascimento, Silvania da Silva Teixeira, Juan Pablo Nicola, Renato Tadeu Nachbar, Ana Maria Masini-Repiso, and Maria Tereza Nunes.

Supplemental Material and Methods

Cell viability and DNA fragmentation assay. Cell viability was analyzed as previous described (28). Briefly, PCCl3 cells were treated with 10^{-3} M sodium iodide for 1 h, the longest period of treatment used in this study. To assess plasma membrane integrity cells were trypsinized and re-suspended in 500 µl PBS containing 50 µl of 20 µg/ml propidium iodide. To evaluated DNA fragmentation, PCCl3 cells were treated with a lysis buffer intended to disrupt the plasma membrane and allow propidium iodide to bind to intact DNA. Ten thousand events were analyzed per condition were evaluated using a FACSCalibur Flow Cytometer (Becton–Dickinson, San Juan, CA, USA). Data was analyzed using Cell Quest Software (Becton–Dickinson, San Juan, CA, USA).

Supplemental Figures Legends

Figure 1 – ***Change in osmolarity does not induce Akt phosphorylation in PCCl3 cells.*** Western blotting analysis of Akt phosphorylation (p-Akt) in PCCl3 cells treated with 10^{-3} M NaCl for different periods of time (15 to 60 min). GAPDH was used for assessing equal loading. Immunoblots shown are representative of two independent experiments. Results are expressed as means ± SEM in arbitrary units (AU). P> 0.05 (*ANOVA, Student–Newman–Keuls*).

Figure 2 – ***I⁻ induces Akt phosphorylation in starved PCCl3 cells.*** Western blotting analysis of Akt phosphorylation (p-Akt) in PCCl3 cells cultured under starving condition for 5 days and treated with 10^{-3} M NaI for 30 min. GAPDH was used as loading control. Immunoblots shown are representative of at least two independent experiments. Results are expressed as mean ± SEM in arbitrary units (AU).* P< 0.05 vs. Basal;••• P< 0.001 vs. Basal+I_{30min}(*ANOVA, Student–Newman–Keuls*).

Figure 3 – ***ROS production is stimulated by low concentrations of I⁻.*** PCCl3 cells previously incubated with the fluorescent dye DHE (5 µM), were treated with 10^{-3} to 10^{-6} M NaI for 30 min. ROS production was evaluated under a rhodamine filter in a common fluorescence ZEISS Axiovert 100 M Microscope and Image-Pro Plus software. Pictures are representative of two independent experiments performed in triplicate.

Figure 4 – ***I⁻ excess does not impair plasma membrane integrity and DNA fragmentation in PCCl3 cells.*** Membrane integrity and DNA fragmentation were evaluated in PCCl3 cells treated with 10^{-3} M NaI for 1 h by flow cytometry, using propidium iodide. Results are representative of two independent experiments performed in triplicate. **A.** M1 and the M2 axis represent cells containing fragmented or intact DNA, respectively. DNA integrity was preserved after iodide excess treatment. P> 0.05 (unpaired two-tailed Student's t-test). **B.** M1 axis represents the number of cells with intact plasma membrane, whereas M2 axis shows cells with altered plasma membrane integrity. No alteration of PCCl3 plasma membrane integrity was induced by iodide excess treatment. P> 0.05 (unpaired two-tailed Student's t-test).

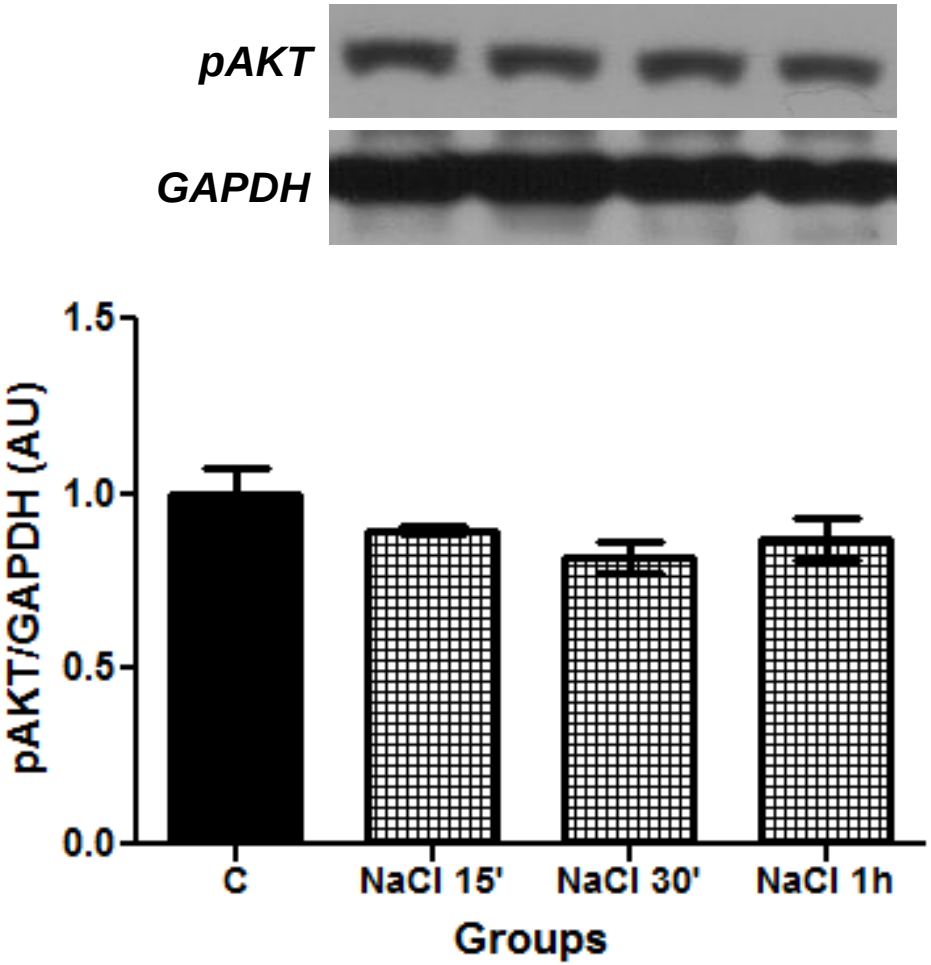
pAKT
GAPDH
1.5
1.0
0.5
0.0
pAKT/GAPDH (AU)
C
NaCl 15'
NaCl 30'
NaCl 1h
Groups

FIGURE – S1

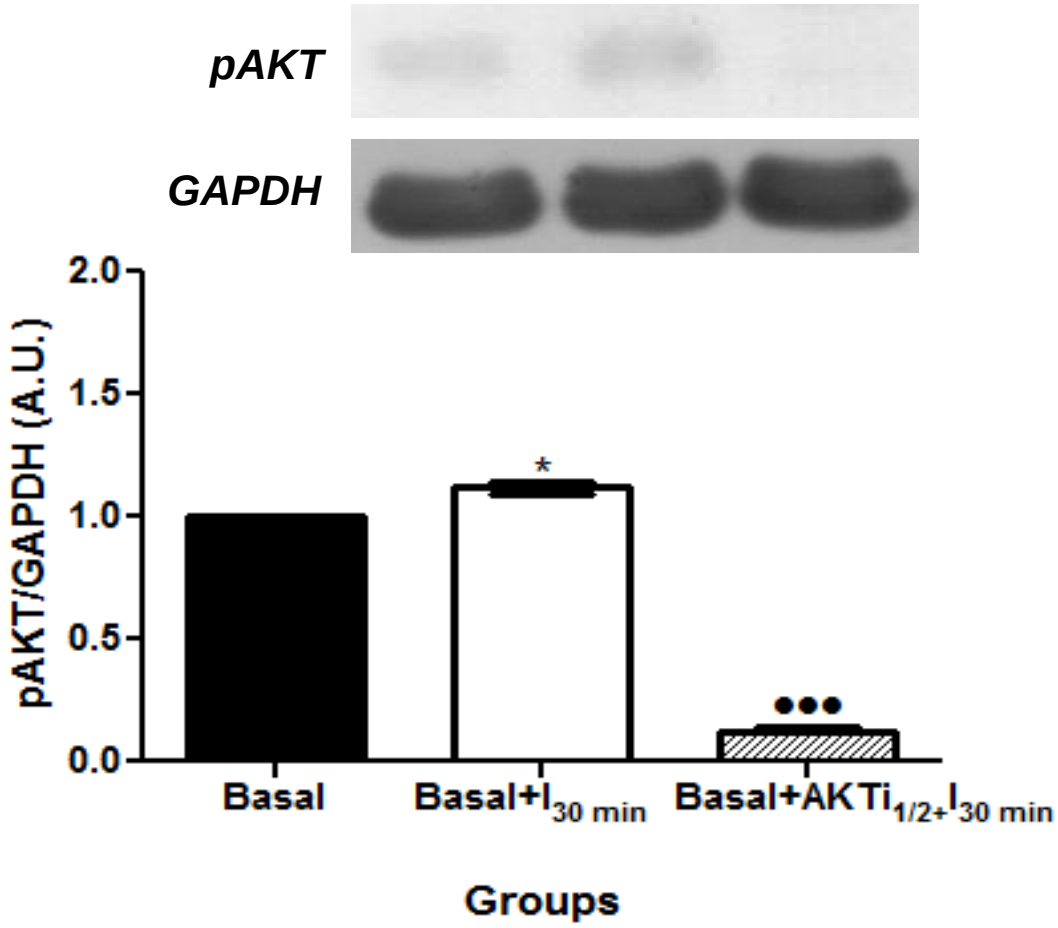
pAKT
GAPDH
2.0
1.5
1.0
0.5
0.0
pAKT/GAPDH (A.U.)
*
Basal
Basal+I30 min
Basal+AKTi1/2+I30 min
Groups

FIGURE – S2

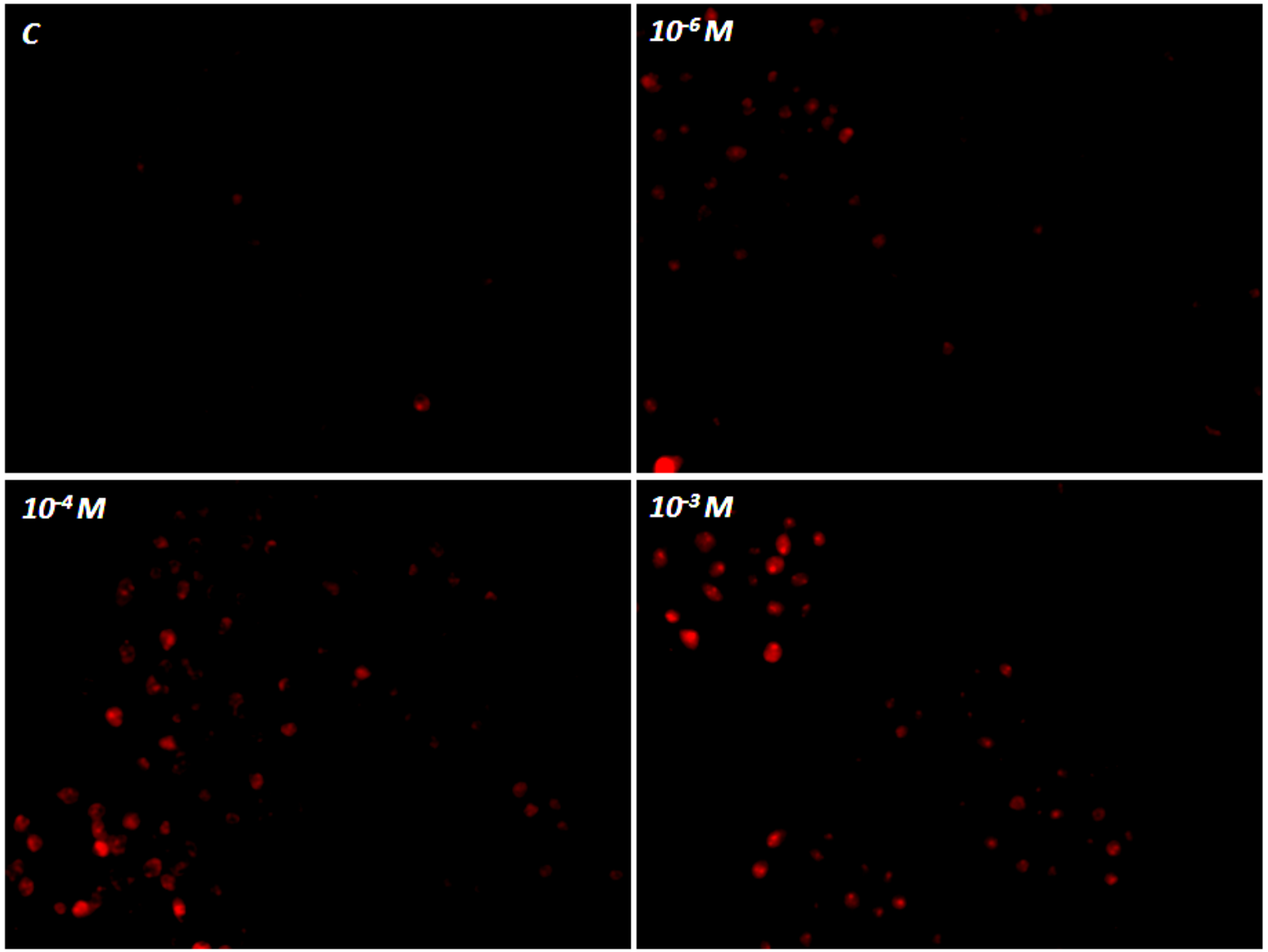

FIGURE – S3

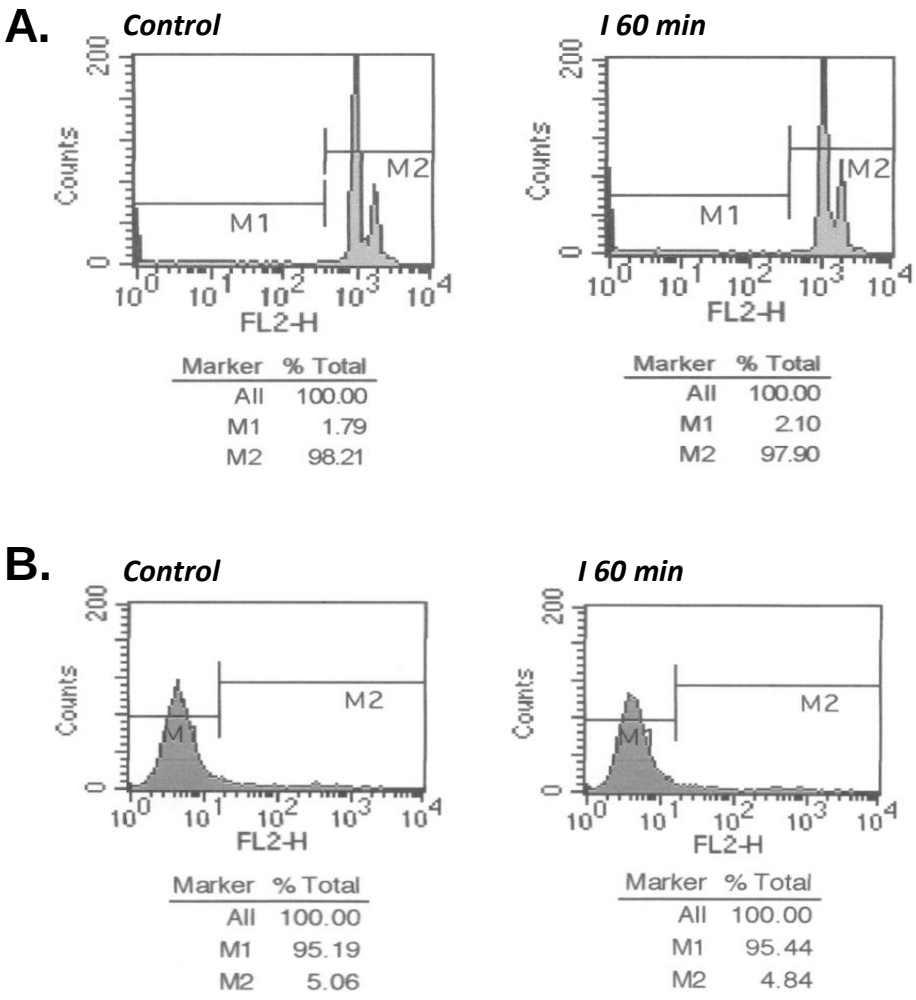
A.
Control
I 60 min
Counts
FL2-H
M1
M2
Marker % Total
All 100.00
M1 1.79
M2 98.21
Marker % Total
All 100.00
M1 2.10
M2 97.90
B.
Control
I 60 min
Counts
FL2-H
M1
M2
Marker % Total
All 100.00
M1 95.19
M2 5.06
Marker % Total
All 100.00
M1 95.44
M2 4.84

FIGURE – S4

SUPPLEMENTAL TABLE: Primers information

Supplemental Table 1 – Primer sets used for NIS mRNA expression analysis in PCCl3 cells by Real-Time PCR.

Gene	Primer	GenBank Reference
RPL19	FWD - 5′-GGCCCGCAAGAAGCTACTG-3′ REV - 5′-TTTCGTGCTTCCTTGGTCTTAGA-3′	NM_031103
Slc5a5 (NIS)	FWD – 5´-AGCCTCGCTCAGAACCATTC-3´ REV – 5´-GTGTACCGGCTCCGAGGAT-3´	NM_052983